HHS Public Access

Author manuscript

ACS Nano. Author manuscript; available in PMC 2016 October 03.

Published in final edited form as:

ACS Nano. 2015 August 25; 9(8): 7775–7782. doi:10.1021/acsnano.5b01696.

Nanoparticle Stabilized Capsules for the Treatment of Bacterial Biofilms

Bradley Duncan[a,†], **Xiaoning Li**[a,†], **Ryan F. Landis**[a], **Sung Tae Kim**[a], **Akash Gupta**[a], **Li-Sheng Wang**[a], **Rajesh Ramanathan**[a,b], **Rui Tang**[a], **Jeffrey A. Boerth**[a], and **Vincent M. Rotello**[a,*]

[a]Department of Chemistry, University of Massachusetts Amherst, 710 North Pleasant Street, Amherst, MA 01003, USA

[b]Ian Potter NanoBioSensing Facility and NanoBiotechnology Research Laboratory, School of Applied Sciences, RMIT University, GPO Box 2476 V, Melbourne, VIC 3001, Australia

Abstract

Bacterial biofilms are widely associated with persistent infections. High resistance to conventional antibiotics and prevalent virulence makes eliminating these bacterial communities challenging therapeutic targets. We describe here the fabrication of a nanoparticle-stabilized capsule with a multicomponent core for the treatment of biofilms. The peppermint oil and cinnamaldehyde combination that comprises the core of the capsules act as potent antimicrobial agents. An *in situ* reaction at the oil/water interface between the nanoparticles and cinnamaldehyde structurally augments the capsules to efficiently deliver the essential oil payloads, effectively eradicating biofilms of clinically isolated pathogenic bacteria strains. In contrast to their antimicrobial action, the capsules selectively promoted fibroblast proliferation in a mixed bacteria/mammalian cell system making them promising for wound healing applications.

Graphical Abstract

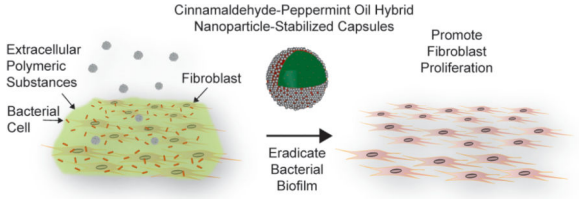

Keywords

Pickering Emulsion; Biofilm; Self-Assembly; Silica Nanoparticles; Phytochemicals

Bacterial biofilms are highly resilient microbial assemblies that are difficult to eradicate.[1] These robust biofilms frequently occur on synthetic implants and indwelling medical devices

* rotello@chem.umass.edu.
† These authors contributed equally to the work.

Supporting Information Available: This material is available free of charge *via* the Internet at http://pubs.acs.org.

including urinary catheters,[2] arthro-prostheses,[3] and dental implants.[4] Biofilm proliferation can also occur on dead or living tissues, leading to endocarditis,[5] otitis media,[6] and chronic wounds.[7] The persistent infections and their concomitant diseases are challenging to treat, as biofilms develop a high resistance to host immune responses and the extracellular polymeric substances limit antibiotic penetration into biofilms.[8,9] Current techniques to remove biofilms on man-made surfaces include disinfecting the surface with bleach or other caustic agents.[10] Biofilms in biomedical contexts are very challenging, with therapies based on excising infected tissues combined with long-term antibiotic therapy, incurring high health care costs and low patient compliance due to the invasive treatment.[11] This issue is exacerbated by the exponential rise in antibiotic resistant bacteria.[12]

Phytochemicals have emerged as an promising alternative to traditional antimicrobials to treat antibiotic resistant bacteria.[13,14] These essential oils and natural compounds are of particular interest as “green” antimicrobial agents due to their low-cost, biocompatibility, and potential anti-biofilm properties.[15,16,17] The generally poor aqueous solubility and stability of these oils has substantially limited their widespread application.[18] Engineering nanomaterials provides a potential platform to prevent payload degradation and to tune molecular interactions with bacteria.[19,20,21,22] Previous reports have shown that encapsulating essential oils into surfactant-stabilized colloidal delivery vehicles improves their aqueous stability and increases the antimicrobial activity of small molecule payloads.[23,24,25] However, these carriers often induce adverse hemolytic or irritating effects restricting their compatibility with biological tissues.[26,27] Pickering emulsions provide an analogous route to encapsulate hydrophobic molecules within a self-assembled colloidal shell that is highly resistant to coalescence.[28,29] The multivalent nanoparticles embedded at the oil/water interface can also be post-functionalized to create structurally diverse carriers not achievable when using surfactant stabilized emulsions.[30,31]

Herein, we describe the fabrication of a multifunctional essential oil-based Pickering emulsion for the treatment of bacterial biofilms. The self-assembly strategy relies on hydrophobic phytochemicals playing both antimicrobial and structural roles for the drug delivery vehicle. Peppermint oil droplets provide the main hydrophobic core template for nanoparticle assembly. Dissolved cinnamaldehyde plays a dual role within the oil core by covalently reacting with the nanoparticles at the interface to modify the shell of the capsules from within and acting as a potent antimicrobial agent once delivered into the biofilm. These microcapsules effectively eradicate both laboratory and pathogenic biofilms. The inclusion of cinnamaldehyde also enhanced fibroblast proliferation[32] promoting therapeutic behavior of the capsules as demonstrated in an *in vitro* co-culture model. This work presents a versatile colloidal strategy for multicomponent essential oil formulations with potential use as a general topical antimicrobial and disinfectant.

Results and Discussion

Generation and characterization of capsules

Silica nanoparticles (SiO_2 NPs) were chosen to stabilize the emulsions as they are biocompatible, surface functionalization can be easily introduced, and their diameters can be readily tuned.[31,33,34] Control over the size of the precursor particles is especially important

as nanomaterials smaller than 70 nm have been shown to readily penetrate the skin causing detrimental side effects.[35,36,37] Therefore, we synthesized cationic amine-functionalized SiO_2 NPs with an average diameter of ~150 nm. (Figure S1–3) Antimicrobial capsules were generated using a Pickering emulsion template as shown in Scheme 1. Capsules were created by emulsifying either peppermint oil or a mixture of cinnamaldehyde dissolved in peppermint oil into MilliQ H_2O adjusted to a pH of 10 containing the nanoparticles. The nanoparticles then self-assemble at the oil/water interface to stabilize the peppermint oil droplets. Finally, surface amines on the nanoparticles react with the cinnamaldehyde within the oil phase. Silica loadings in the aqueous phase were varied to determine the amount of NP needed to minimize capsule dispersity. At loadings above of 1.2 wt. % SiO_2 NPs or greater, capsules were found to have a minimum dispersity and therefore this amount was chosen for all further studies. (Figure S4) It was also observed that capsules generated with higher than 5 % v/v cinnamaldehyde (corresponding to 52-fold excess of cinnamaldehyde to available amines on the nanoparticle surface) were unstable. (Figure S5) These peppermint oil based capsules (P-Cap) and capsules containing 5 % v/v of cinnamaldehyde dissolved in peppermint oil (CP-Cap) were found to have average diameters of 6.8 ± 1.9 μm and 6.7 ± 1.9 μm, respectively. (Figure S6)

We used confocal microscopy, X-ray photoelectron spectroscopy (XPS), attenuated total reflection Fourier transform infrared spectroscopy (ATR-FTIR), and contact angle goniometry to probe the cinnamaldehyde-nanoparticle interaction. Reactive molecules within the oil core of Pickering emulsions have been previously demonstrated to affect capsule morphologies by modulating the hydrophobicity of the nanoparticles.[38,39] To determine if structural reorganization occurs with our mixed oil system, capsules were generated using a Nile red loaded oil core and nanoparticles possessing cores labeled with fluorescein isothiocyanate (FITC). As shown in Figure 1a, b, and S7, both capsules with and without cinnamaldehyde possess core-shell morphologies. This result indicates that the 5 % v/v loading of cinnamaldehyde into the peppermint oil does not alter the capsule structure.

We next used XPS and ATR-FTIR to elucidate the reactivity of the nanoparticles with the dissolved cinnamaldehyde of the capsules. Prior to analysis, CP-Caps were disrupted with ethanol, centrifuged, and lyophilized to remove any adsorbed cinnamaldehyde. The Schiff base of 3-aminopropyltriethoxysilane and cinnamaldehyde was also synthesized for comparison. (Figure S8) As shown in Figure 1c, the SiO_2 NPs showed two chemically distinct species with a lower binding energy (BE) component at ca. 399.5 eV and a higher BE component at ca. 401.8 eV. These correspond to amine (-NH-) and protonated amine (NH_3^+) present on the surface of SiO_2 NPs that is consistent with previously reported values.[40] The N 1s spectra of CP-Cap shows three distinct chemical species. In addition to the two N 1s BE components observed in the SiO_2 NPs, a new peak centered at ca. 400.1 eV indicates the formation of an imine functional (-C=N-) group which corroborates well with literature values.[41] (Figure 1c) The N 1s spectra from the synthesized Schiff base (Figure S9) showed a single chemically distinct N 1s species centered at ca. 400.2 eV, which corresponds to the imine functional group (-C=N-).[41] Similarly, the chemically distinct species of the C 1s spectra obtained from CP-Cap matches well with the synthesized Schiff base further providing evidence on the covalent linkage of the amine and cinnamaldehyde (Figure S9). Additionally, the Si 2p and O 1s peak shows typical BEs centered at ca. 103.2

eV and 532.6 eV, respectively that matches with reported values for SiO_2 NPs (Figure S6).[42] ATR-FTIR analysis further supported the formation of the cinnamaldehyde Schiff base (Figure S10).

An *in situ* covalent reaction of the primary amine groups on the nanoparticles with cinnamaldehyde should alter the hydrophobicity of the nanoparticle surface improving the stabilization behavior of the Pickering emulsifiers.[43] (See Supporting Information) Contact angle goniometry was used to measure the change in nanoparticle hydrophobicity. Nanoparticles were deposited onto silicon wafers and briefly incubated in dichloromethane solutions with varying amounts of dissolved cinnamaldehyde. The surfaces were then rinsed with dichloromethane, dried, and the water contact angles were obtained. (Figure S11) Figure 2d shows that as the percentage of cinnamaldehyde by volume increases from 0 % to 5 %, the water contact angle of the nanoparticles increases from 31° to 49°. This increase in water contact angle, taken together with the XPS data, the ATR-FTIR data, and confocal images, indicates that the inclusion of cinnamaldehyde within the peppermint oil core generates a distinct, multi-component capsule structure.

Capsule Penetration into the biofilms

Biofilms produce extracellular polymeric substances that prevent effective delivery of therapeutics.[44] Having established that the capsules have core-shell morphologies and the cinnamaldehyde is successfully incorporated into the capsules, we set out to determine whether these capsules could effectively penetrate into biofilms. Using fluorescently labeled nanoparticles to track the delivery of the emulsions, we treated biofilms from *E. coli* that had been modified to express E2-Crimson, a far-red fluorescent protein. As shown in Figure 2, both P-Cap and CP-Cap diffuse into the biofilm matrix and efficiently disperse throughout the biofilm whereas the unassembled nanoparticles displayed minimal penetration. These data indicate the capsules deliver their payload in a burst release fashion and that both the oil core and nanoparticle shell are operative for effective delivery.

Antimicrobial activity of capsules against biofilms

Next, we investigated the therapeutic behavior of the capsules against established bacterial biofilms. One laboratory strain, *E. coli DH5α*, and 3 pathogenic bacteria strains of clinical isolates, *P. aeruginosa* (CD-1006), *S. aureus* (CD-489, a methicillin-resistant strain), and *E. cloacae complex* (CD-1412), were chosen to test our system. As shown in Figure 3, both the CP-Cap and P-Cap vehicles effectively were able to kill bacteria cells in all four biofilms, with CP-Cap possessing greater activity. The capsules demonstrated a dramatically enhanced efficacy compared with the unencapsulated oil, supporting the hypothesis that the cationic nanoparticle shell of the capsules increases interaction with the biofilms.[45] In addition, the acidic pH of the biofilm environment[46] should promote the hydrolysis of Schiff bases, enhancing the sustained release of cinnamaldehyde. These capsules were able to treat both Gram negative (*E. coli, P. aeruginosa*, and *E. cloacae* complex) and Gram positive (*S. aureus*) bacteria. Notably, the capsules demonstrated a similar efficacy against the multi-drug resistant *S. aureus* stain when compared to the non-resistant strains, supporting that these capsules present a viable treatment alternative to traditional antibiotics.

Co-culture treatment of biofilms

Biofilm infections within wounds interfere with the ability of the host to regenerate damaged tissue.[47] Fibroblasts in particular play a vital role in the wound healing process, helping to close the injury and redevelop the extracellular matrix within the skin.[48,49] We used an *in vitro* co-culture model comprised of mammalian fibroblasts and a biofilm to determine whether our capsules could successfully treat a biofilm in the presence of host cells.[50] *E. coli* DH5α bacteria were seeded with a confluent NIH 3T3 fibroblast cell monolayer overnight to generate biofilms prior to treatment. The co-cultures were treated with capsules for 3 hrs, washed, and the viabilities of both fibroblasts and bacteria were measured. As shown in Figure 4, CP-Cap effectively treated the biofilm infection whereas P-Cap and the controls did not. The capsule structure also prevented the toxic effects shown by the unencapsulated peppermint oil to the fibroblasts. Notably, CP-Cap enhanced 3T3 cell growth in agreement with studies that cinnamaldehyde can promote insulin-like growth factor-I signaling, increasing cell proliferation.[51]

Conclusion

In summary, we report the development of a multimodal antimicrobial delivery vehicle. The nanoparticle stabilized capsules demonstrated highly effective therapeutic behavior, successfully eradicating pathogenic biofilm strains of clinical isolates. Furthermore, the capsules effectively eliminated a biofilm infection while promoting fibroblast viability in an *in vitro* co-culture model. Future studies will probe capsule performance in combating *in vivo* biofilms. These capsules have potential applications as a general surface disinfectant as well as an antiseptic for wound treatment. The reactive self-assembly based strategy provides a promising platform to create effective delivery vehicles to combat bacterial biofilms.

Materials and Methods

All reagents/materials were purchased from Fisher Scientific and used as received. Boron-doped Si wafers were purchased from WRS Materials. NIH-3T3 cells (ATCC CRL-1658) were purchased from ATCC. Dulbecco's Modified Eagle's Medium (DMEM) (DMEM; ATCC 30-2002) and fetal bovine serum (Fisher Scientific, SH3007103) were used in cell culture. Pierce LDH Cytotoxicity Assay Kit was purchased from Fisher Scientific.

Synthesis and functionalization of silica nanoparticles

Silica nanoparticles (See Supporting Information for synthesis and characterization) were synthesized as previously reported.[38]

Preparation of capsules

Stock capsules solutions were prepared in 1.5 mL Eppendorf tubes. To prepare the stock P-Cap emulsions, 300 μL of peppermint oil was added to 1.2 mL of a 1.2 % wt. solution of SiO_2 NPs in MilliQ H_2O adjusted to pH 10 and was emulsified in an amalgamator for 50 seconds. To prepare the stock CP-Cap emulsions, 15 μL of cinnamaldehyde was dissolved in

285 μL of peppermint oil prior to emulsification as described. The emulsions were allowed to rest overnight prior to use.

X-ray photoelectron spectroscopy

Samples were prepared by drop-casting the sample on a 100 nm gold-coated silicon substrate. XPS measurements were carried out using Physical Electronics Quantum 2000 spectrometer at a pressure below 1×10^{-9} Torr. The survey scan, C 1s, N 1s, O 1s and Si 2p core level spectra for all samples were recorded with un-monochromatized Al Kα radiation (photon energy of 1486.6 eV) at a pass energy of 46.95 eV and electron takeoff angle of 15°. The overall resolution was 0.2 eV for the XPS measurements. Chemically distinct species were resolved using a Gaussian-Lorentzian function with non-linear least-square fitting procedure. All XPS spectra were background corrected using the Shirley algorithm and aligning the elemental binding energies to the adventitious carbon (C1s) binding energy of 284.6 eV.[42]

Contact angle goniometry

Samples were prepared by immersing a clean silicon wafer (1 cm × 1 cm) into 1 mL of a 1.2 % wt. solution of SiO_2 NPs in MilliQ H_2O adjusted to pH 10 for 5 minutes. Wafers were then washed with MilliQ H_2O to removed excess nanoparticles and dried under a N_2 stream. Samples were then incubated in 1 mL solutions of dichloromethane with varying amounts (0, 1, 2, 5 % v/v) of dissolved cinnamaldehyde for 5 minutes. Wafers were then washed with dichloromethane and dried under a N_2 stream. Static water contact angles were measured using a VCA Optima surface analysis/goniometry system with water droplets size of 2 μL.

Biofilm formation

Biofilms were grown as previously reported.[50] Bacteria were inoculated in lysogeny broth (LB) medium at 37 °C until stationary phase. The cultures were then harvested by centrifugation and washed with 0.85 % sodium chloride solution three times. Concentrations of resuspended bacterial solution were determined by optical density measured at 600 nm. LB medium was supplemented with 0.1 % glucose, 1 mM $MgSO_4$, 0.15 M ammonium sulfate, and 34 mM citrate and buffered to pH 7 to ensure bacterial adherence to the microplate. Seeding solutions were then made in this modified LB medium to reach an OD_{600} of 0.1. A 100 μL amount of the seeding solutions was added to each well of the 96 well microplate. The plates were covered and incubated at room temperature under static conditions for 1 day.

A 2 % v/v emulsion stock solution made by diluting the generated capsules into LB medium. The stock solution was then diluted to the desired level and incubated with the biofilms for 3 hrs. Biofilms were washed with phosphate buffer saline (PBS) three times and viability was determined using an Alamar Blue assay.[52] Modified LB medium without bacteria was used as a negative control.

Biofilm-3T3 fibroblast cell co-culture

Co-culture was performed as previously described.[50] Briefly, a total of 20,000 NIH 3T3 (ATCC CRL-1658) cells were cultured in Dulbecco's modified Eagle medium (DMEM;

ATCC 30-2002) with 10 % bovine calf serum and 1% antibiotics at 37 °C in a humidified atmosphere of 5 % CO_2. Cells were kept for 24 h to reach a confluent monolayer. Bacteria were inoculated and harvested as described above, and seeding solutions were made in buffered DMEM supplemented with glucose to reach an OD_{600} of 0.1. Old medium was removed from 3T3 cells followed by addition of 100 μL of seeding solution. The co-cultures were then stored in a box with damp paper towels at 37 °C overnight without shaking.

Testing solutions at different concentrations were made by diluting capsules into DMEM prior to use. Media was removed from co-culture, replaced with testing solutions, and incubated for 3 hrs at 37 °C. Co-cultures were then analyzed using a LDH cytotoxicity assay to determine mammalian cell viability according the manufacturer's instructions.[53] To determine bacteria viability in biofilms, the testing solutions were removed and co-cultures were washed with PBS. Fresh PBS was then added to disperse remaining bacteria from biofilms in co-culture by sonication for 20 minutes and mixing with pipette. The solutions containing dispersed bacteria were then plated onto agar plates and colony forming units were counted after incubation at 37 °C overnight.

Supplementary Material

Refer to Web version on PubMed Central for supplementary material.

Acknowledgments

This research was supported by Firmenich SA, the NIH (EB014277) and the NSF Center for Hierarchical Manufacturing, CMMI-1025020. Clinical samples were kindly provided to Dr. Margaret Riley by the Cooley Dickinson Hospital Microbiology Laboratory (Northampton, MA).

References

1. Costerton JW, Stewart PS, Greenburg EP. Bacterial Biofilms: A Common Cause of Persistent Infections. Science. 1999; 284:1318–1322. [PubMed: 10334980]
2. Lindsay D, von Holy A. Bacterial Biofilms within the Clinical Setting: What Healthcare Professionals Should Know. J. Hosp. Infect. 2006; 64:313–325. [PubMed: 17046102]
3. Costerton JW, Montanaro L, Arciola CR. Biofilm in Implant Infections: Its Production and Regulation. Int. J. Artif. Organs. 2005; 28:1062–1068. [PubMed: 16353112]
4. Busscher HJ, Rinastiti M, Siswomihardjo W, van der Mei HC. Biofilm Formation on Dental Restorative and Implant Materials. J. Dent. Res. 2010; 89:657–665. [PubMed: 20448246]
5. Costerton W, Veeh R, Shirtliff M, Pasmore M, Post C, Ehrlich G. The Application of Biofilm Science to the Study and Control of Chronic Bacterial Infections. J. Clin. Invest. 2003; 112:1466–1477. [PubMed: 14617746]
6. Ehrlich G, Veeh R, Wang X, Costerton JW, Hayes JD, Hu FZ, Daigle BJ, Ehrlich MD, Post JC. Mucosal Biofilm Formation on Middle-Ear Mucosa in the Chinchilla Model of Otitis Media. JAMA. 2002; 287:1710. [PubMed: 11926896]
7. James GA, Swogger E, Wolcott R, Pulcini E deLancey, Secor P, Sestrich J, Costerton JW, Stewart PS. Biofilms in Chronic Wounds. Wound Repair Regen. 2007; 16:37–44. [PubMed: 18086294]
8. Stewart PS, Costerton JW. Antibiotic Resistance of Bacteria in Biofilms. Lancet. 2001; 358:135–138. [PubMed: 11463434]
9. Szomolay B, Klapper I, Dockery J, Stewart PS. Adaptive Responses to Antimicrobial Agents in Biofilms. Environ. Microbiol. 2005; 7:1186–1191. [PubMed: 16011755]

10. Marion-Ferey K, Pasmore M, Stoodley P, Wilson S, Husson GP, Costerton JW. Biofilm Removal from Silicone Tubing: An Assessment of the Efficacy of Dialysis Machine Decontamination Procedures Using an *in Vitro* Model. J. Hosp. Infect. 2003; 53:64–71. [PubMed: 12495687]
11. Lynch AS, Robertson GT. Bacterial and Fungal Biofilm Infections. Annu. Rev. Med. 2008; 59:415–428. [PubMed: 17937586]
12. Levy SB, Marshall B. Antibacterial Resistance Worldwide: Causes, Challenges and Responses. Nat. Med. 2004; 10:S122–S129. [PubMed: 15577930]
13. Kalemba D, Kunicka A. Antibacterial and Antifungal Properties of Essential Oils. Curr. Med. Chem. 2003; 10:813–829. [PubMed: 12678685]
14. Hemaiswarya S, Kruthiventi AK, Doble M. Synergism between Natural Products and Antibiotics against Infectious Diseases. Phytomedicine. 2008; 15:639–652. [PubMed: 18599280]
15. Burt S. Essential Oils: Their Antibacterial Properties and Potential Applications in Foods--a Review. Int. J. Food Microbiol. 2004; 94:223–253. [PubMed: 15246235]
16. Kavanaugh NL, Ribbeck K. Selected Antimicrobial Essential Oils Eradicate *Pseudomonas Spp* and *Staphylococcus Aureus* Biofilms. Appl. Environ. Microbiol. 2012; 78:4057–4061. [PubMed: 22467497]
17. Nostro A, Sudano Roccaro A, Bisignano G, Marino A, Cannatelli MA, Pizzimenti FC, Cioni PL, Procopio F, Blanco AR. Effects of Oregano, Carvacrol and Thymol on *Staphylococcus Aureus* and *Staphylococcus Epidermidis* Biofilms. J. Med. Microbiol. 2007; 56:519–523. [PubMed: 17374894]
18. Chen H, Davidson PM, Zhong Q. Impacts of Sample Preparation Methods on Solubility and Antilisterial Characteristics of Essential Oil Components in Milk. Appl. Environ. Microbiol. 2014; 80:907–916. [PubMed: 24271170]
19. Carpenter AW, Worley BV, Slomberg DL, Schoenfisch MH. Dual Action Antimicrobials: Nitric Oxide Release from Quaternary Ammonium-Functionalized Silica Nanoparticles. Biomacromolecules. 2012; 13:3334–3342. [PubMed: 22998760]
20. Zhu X, Radovic-Moreno AF, Wu J, Langer R, Shi J. Nanomedicine in the Management of Microbial Infection - Overview and Perspectives. Nano Today. 2014; 9:478–498. [PubMed: 25267927]
21. Radovic-Moreno AF, Lu TK, Puscasu Va, Yoon CJ, Langer R, Farokhzad OC. Surface Charge-Switching Polymeric Nanoparticles for Bacterial Cell Wall-Targeted Delivery of Antibiotics. ACS Nano. 2012; 6:4279–4287. [PubMed: 22471841]
22. Goswami S, Thiyagarajan D, Das G, Ramesh A. Biocompatible Nanocarrier Fortified with a Dipyridinium-Based Amphiphile for Eradication of Biofilm. ACS Appl. Mater. Interfaces. 2014; 6:16384–16394. [PubMed: 25162678]
23. Chang Y, McLandsborough L, McClements DJ. Physicochemical Properties and Antimicrobial Efficacy of Carvacrol Nanoemulsions Formed by Spontaneous Emulsification. J. Agric. Food Chem. 2013; 61:8906–8913. [PubMed: 23998790]
24. Liang R, Xu S, Shoemaker CF, Li Y, Zhong F, Huang Q. Physical and Antimicrobial Properties of Peppermint Oil Nanoemulsions. J. Agric. Food Chem. 2012; 60:7548–7555. [PubMed: 22746096]
25. Gomes C, Moreira RG, Castell-Perez E. Poly (DL-Lactide-Co-Glycolide) (PLGA) Nanoparticles with Entrapped Trans-Cinnamaldehyde and Eugenol for Antimicrobial Delivery Applications. J. Food Sci. 2011; 76:N16–N24. [PubMed: 21535781]
26. Shalel S, Streichman S, Marmur A. The Mechanism of Hemolysis by Surfactants: Effect of Solution Composition. J. Colloid Interface Sci. 2002; 252:66–76. [PubMed: 16290763]
27. Wilhelm K-P, Freitag G, Wolff HH. Surfactant-Induced Skin Irritation and Skin Repair. J. Am. Acad. Dermatol. 1994; 30:944–949. [PubMed: 8188884]
28. Ramsden W. Separation of Solids in the Surface-Layers of Solutions and “Suspensions” (Observations on Surface-Membranes, Bubbles, Emulsions, and Mechanical Coagulation). -- Preliminary Account. Proc. R. Soc. London. 1903; 72:156–164.
29. Pickering SU. Emulsions. J. Chem. Soc. Trans. 1907; 91:2001.
30. Binks BP. Particles as Surfactants—Similarities and Differences. Curr. Opin. Colloid Interface Sci. 2002; 7:21–41.

31. Ghouchi Eskandar N, Simovic S, Prestidge CA. Nanoparticle Coated Submicron Emulsions: Sustained in-Vitro Release and Improved Dermal Delivery of All-Trans-Retinol. Pharm. Res. 2009; 26:1764–1775. [PubMed: 19384464]
32. Takasao N, Tsuji-Naito K, Ishikura S, Tamura A, Akagawa M. Cinnamon Extract Promotes Type I Collagen Biosynthesis *via* Activation of IGF-I Signaling in Human Dermal Fibroblasts. J. Agric. Food Chem. 2012; 60:1193–1200. [PubMed: 22233457]
33. Stöber W, Fink A, Bohn E. Controlled Growth of Monodisperse Silica Spheres in the Micron Size Range. Journal of Colloid and Interface Science. 1968; 26:62–69.
34. Rosen JE, Gu FX. Surface Functionalization of Silica Nanoparticles with Cysteine: A Low-Fouling Zwitterionic Surface. Langmuir. 2011; 27:10507–10513. [PubMed: 21761888]
35. Rancan F, Gao Q, Graf C, Troppens S, Hadam S, Hackbarth S, Kembuan C, Blume-Peytavi U, Rühl E, Lademann J, et al. Skin Penetration and Cellular Uptake of Amorphous Silica Nanoparticles with Variable Size, Surface Functionalization, and Colloidal Stability. ACS Nano. 2012; 6:6829–6842. [PubMed: 22797484]
36. Labouta HI, Schneider M. Interaction of Inorganic Nanoparticles with the Skin Barrier: Current Status and Critical Review. Nanomedicine: Nanotechnology, Biology, and Medicine. 2013; 9:39–54.
37. Nabeshi H, Yoshikawa T, Matsuyama K, Nakazato Y, Matsuo K, Arimori A, Isobe M, Tochigi S, Kondoh S, Hirai T, et al. Systemic Distribution, Nuclear Entry and Cytotoxicity of Amorphous Nanosilica Following Topical Application. Biomaterials. 2011; 32:2713–2724. [PubMed: 21262533]
38. Duncan B, Landis RF, Jerri Ha, Normand V, Benczédi D, Ouali L, Rotello VM. Hybrid Organic-Inorganic Colloidal Composite “Sponges” *via* Internal Crosslinking. Small. 2015; 11:1302–1309. [PubMed: 25381874]
39. Williams M, Warren NJ, Fielding LA, Armes SP, Verstraete P, Smets J. Preparation of Double Emulsions Using Hybrid Polymer/Silica Particles: New Pickering Emulsifiers with Adjustable Surface Wettability. ACS Appl. Mater. Interfaces. 2014; 6:20919–20927. [PubMed: 25380488]
40. Tan K, Tan B, Kang E, Neoh K. X-Ray Photoelectron Spectroscopy Studies of the Chemical Structure of Polyaniline. Phys. Rev. B. 1989; 39:8070–8073.
41. Ricci M, Trinquecoste M, Auguste F, Canet R, Delhaes P, Guimon C, Pfister-Guillouzo G, Nysten B, Issi JP. Relationship between the Structural Organization and the Physical Properties of PECVD Nitrogenated Carbons. J. Mater. Res. 1993; 8:480–488.
42. Ramanathan R, Campbell JL, Soni SK, Bhargava SK, Bansal V. Cationic Amino Acids Specific Biomimetic Silicification in Ionic Liquid: A Quest to Understand the Formation of 3-D Structures in Diatoms. PLoS One. 2011; 6
43. Pieranski P. Two-Dimensional Interfacial Colloidal Crystals. Phys. Rev. Lett. 1980; 45:569–572.
44. Hurdle JG, O’Neill AJ, Chopra I, Lee RE. Targeting Bacterial Membrane Function: An Underexploited Mechanism for Treating Persistent Infections. Nat. Rev. Microbiol. 2011; 9:62–75. [PubMed: 21164535]
45. Li X, Yeh Y, Giri K, Mout R, Landis RF, Prakash YS, Rotello VM. Control of Nanoparticle Penetration into Biofilms through Surface Design. Chem. Commun. (Camb). 2015; 51:282–285. [PubMed: 25407407]
46. Harrison JJ, Ceri H, Turner RJ. Multimetal Resistance and Tolerance in Microbial Biofilms. Nat. Rev. Microbiol. 2007; 5:928–938. [PubMed: 17940533]
47. Roy S, Elgharably H, Sinha M, Ganesh K, Chaney S, Mann E, Miller C, Khanna S, Bergdall VK, Powell HM, et al. Mixed-Species Biofilm Compromises Wound Healing by Disrupting Epidermal Barrier Function. J. Pathol. 2014; 233:331–343. [PubMed: 24771509]
48. Watt FM. Mammalian Skin Cell Biology: At the Interface between Laboratory and Clinic. Science. 2014; 346:937–940. [PubMed: 25414300]
49. Sun BK, Siprashvili Z, Khavari PA. Advances in Skin Grafting and Treatment of Cutaneous Wounds. Science. 2014; 346:941–945. [PubMed: 25414301]
50. Li X, Kong H, Mout R, Saha K, Moyano DF, Robinson SM, Rana S, Zhang X, Riley MA, Rotello VM. Rapid Identification of Bacterial Biofilms and Biofilm Wound Models Using a Multichannel Nanosensor. ACS Nano. 2014; 8:12014–12019. [PubMed: 25454256]

51. Takasao N, Tsuji-Naito K, Ishikura S, Tamura A, Akagawa M. Cinnamon Extract Promotes Type I Collagen Biosynthesis via Activation of IGF-I Signaling in Human Dermal Fibroblasts. J. Agric. Food Chem. 2012; 60:1193–1200. [PubMed: 22233457]

52. Margarida Pereira A, Cristina Abreu A, Simões M. Action of Kanamycin Against Single and Dual Species Biofilms of *Escherichia Coli and Staphylococcus Aureus*. J. Microbiol. Res. 2012; 2:84–88.

53. Decker T, Lohmann-Matthes ML. A Quick and Simple Method for the Quantitation of Lactate Dehydrogenase Release in Measurements of Cellular Cytotoxicity and Tumor Necrosis Factor (TNF) Activity. J. Immunol. Methods. 1988; 115:61–69. [PubMed: 3192948]

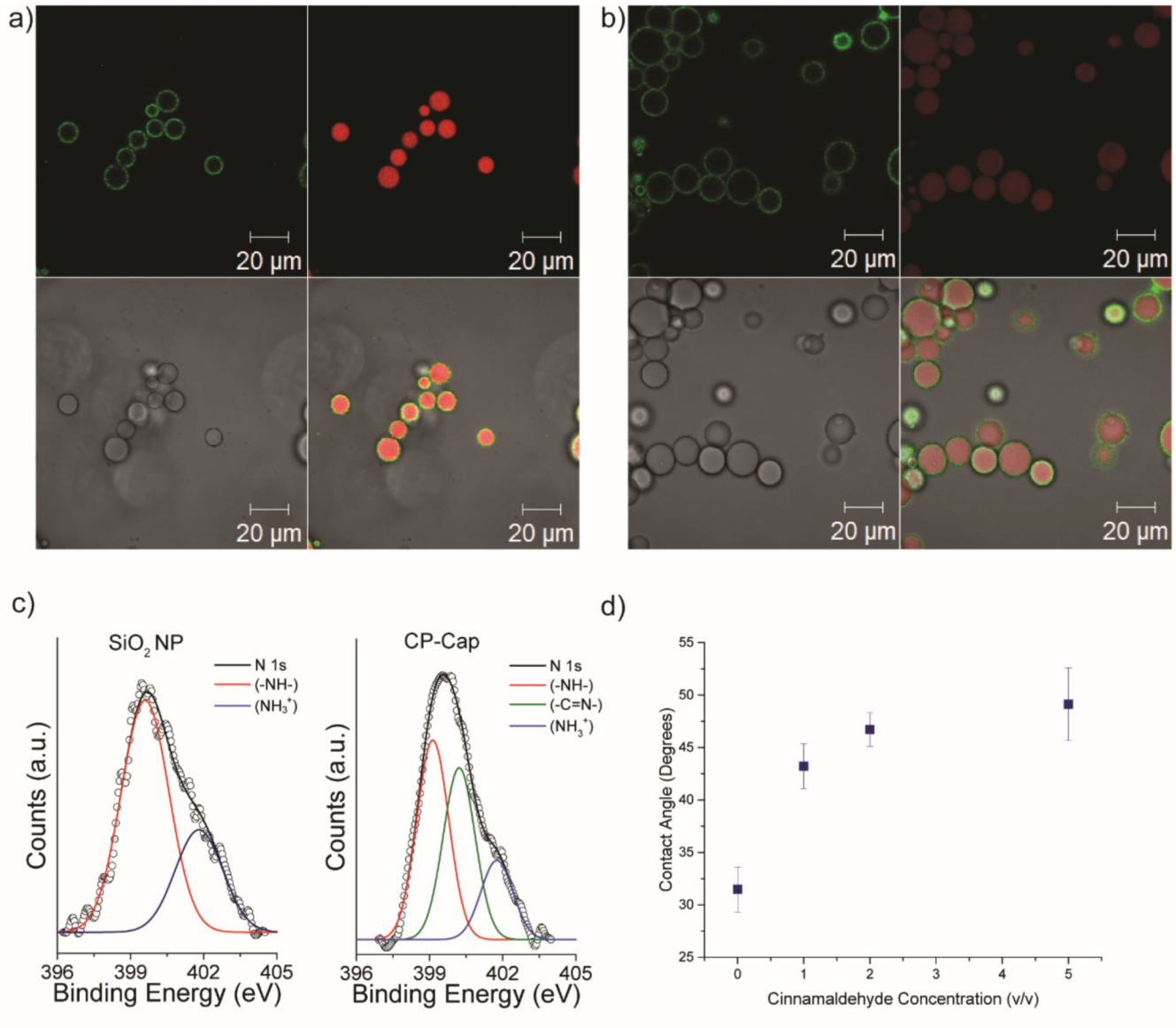

Figure 1.

Confocal micrographs of a) P-Cap and b) CP-Cap. The nanoparticles' cores are labeled with fluorescein (green fluorescence) and the oil phases are loaded with Nile red (red fluorescence). Scale bars are 20 μm. c) XPS spectra showing N 1s core levels arising from SiO_2 NPs and CP-Cap. d) Water contact angles of silica nanoparticles following incubation with varying concentrations of cinnamaldehyde.

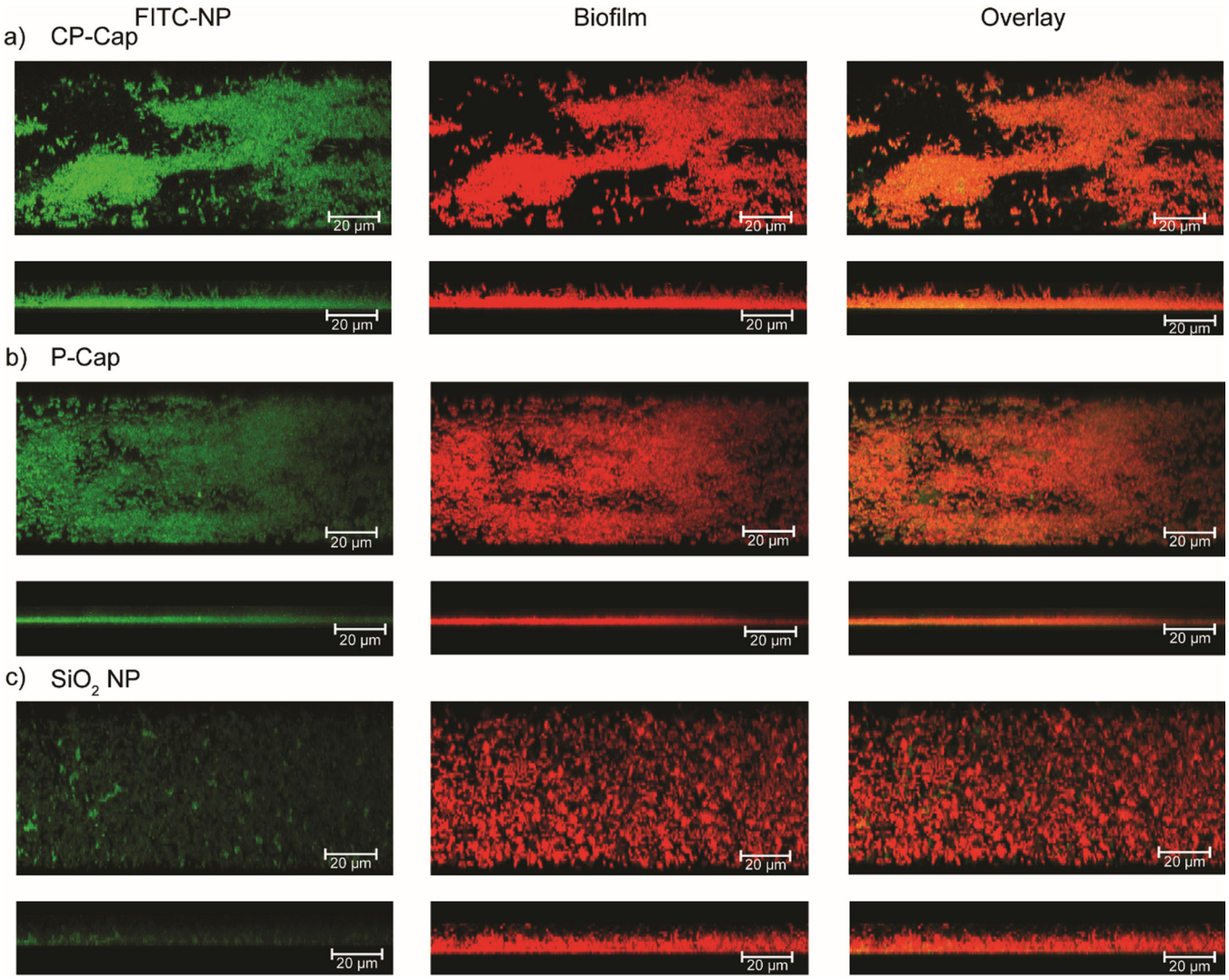

Figure 2.

Representative 3D projection of confocal image stacks of 1 day-old *E. coli DH5α* biofilm after 3 hrs treatment with a) CP-Cap containing FITC-labeled SiO2 NP, b) P-Cap containing FITC-labeled SiO_2 NP, and c) FITC-labeled SiO_2 NP at 20 % (v/v % of 2 % emulsion) concentration. Upper panels are projection at 247° angle turning along Y axis and lower panels are at 270° angle turning along Y axis. Scale bars are 20 μm.

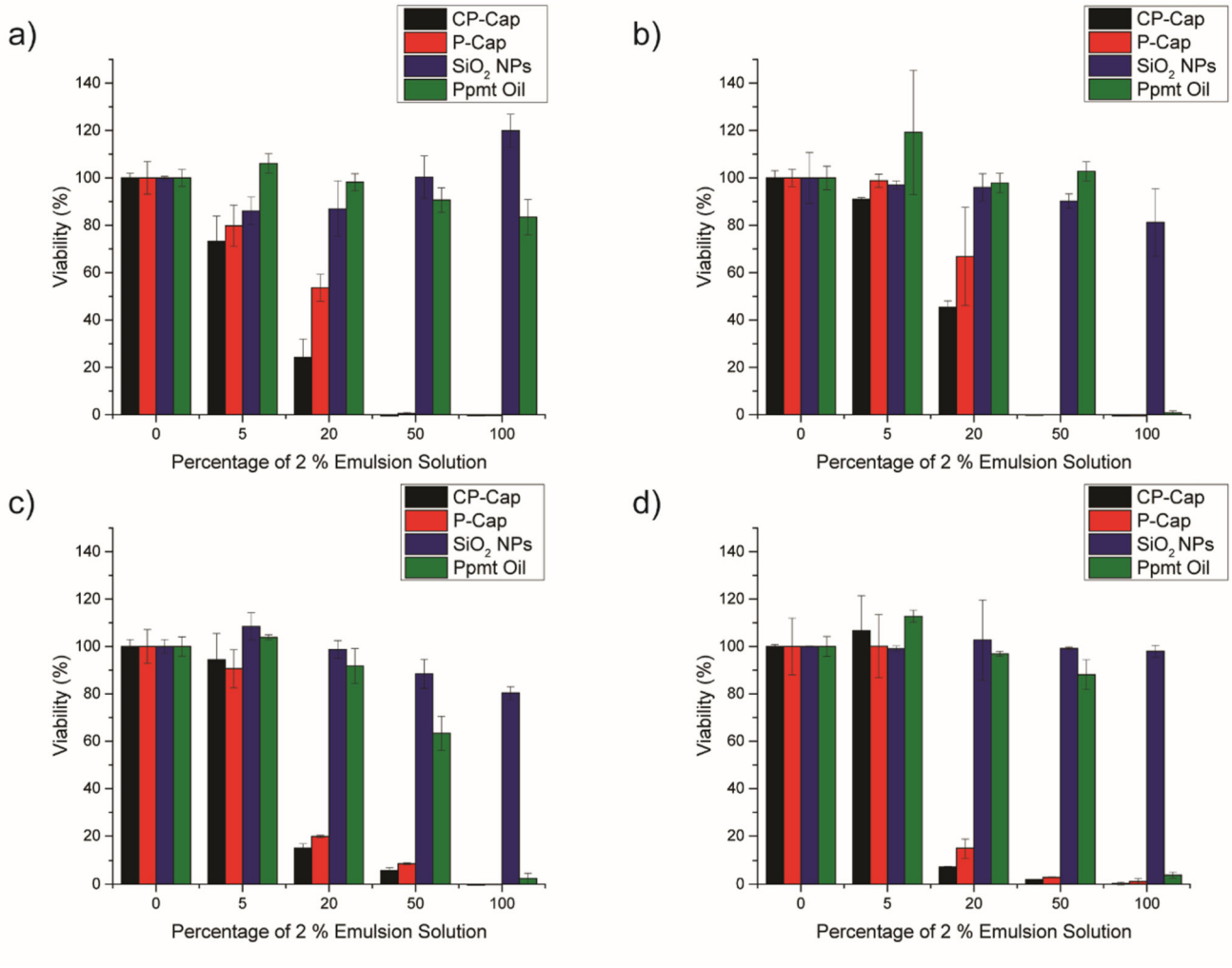

Figure 3.

Viability of 1 day-old a) *P. aeruginosa* (CD-1006) b) *E. coli* DH5α c) *S. aureus* (CD-489) d) *E. cloacae* complex (CD-1412) biofilms after 3 hrs treatment with CP-Cap, P-Cap, SiO2 NP, and peppermint oil at different emulsion concentrations (v/v % of 2 % emulsion). The data are average of triplicates and the error bars indicate the standard deviations.

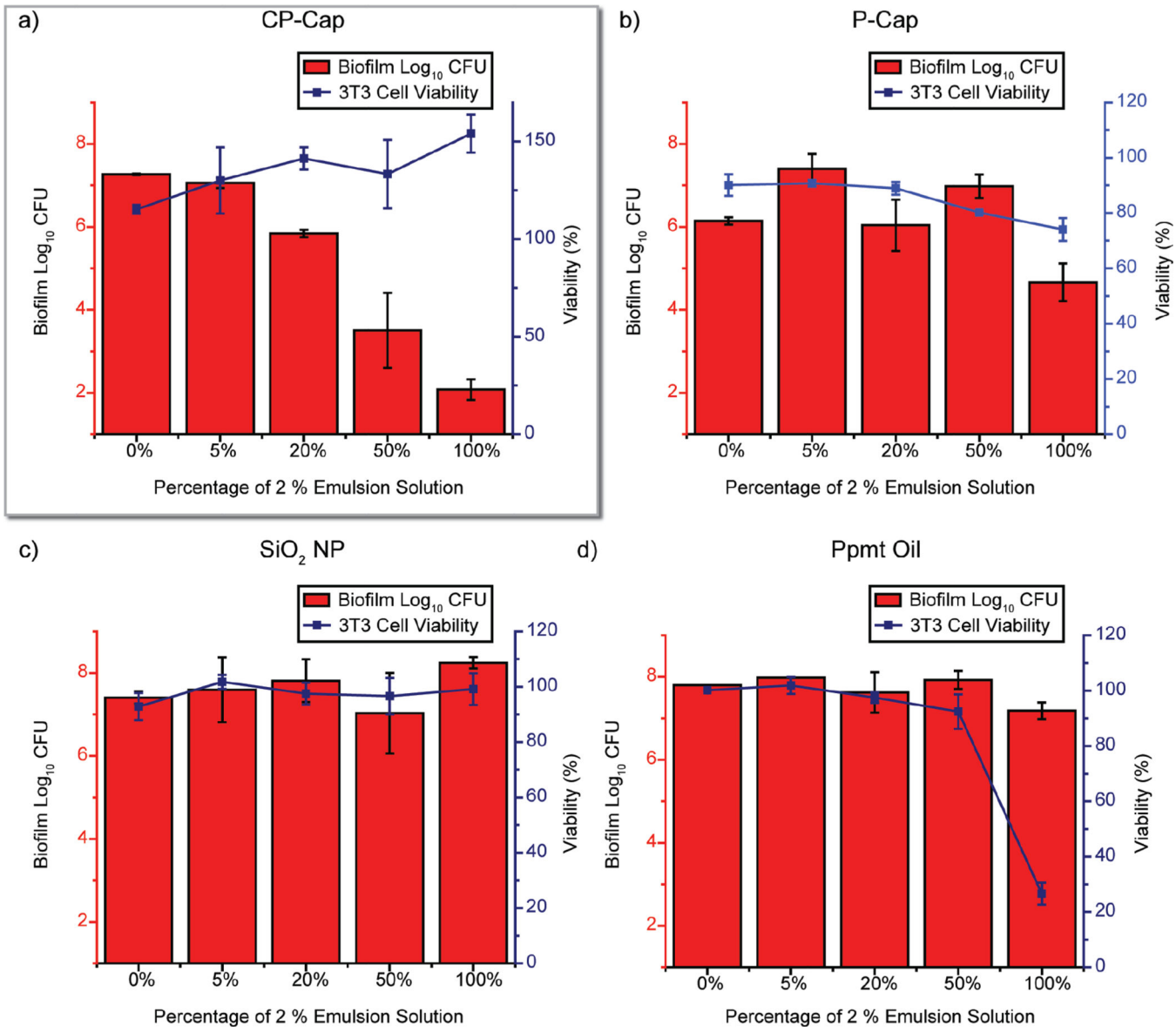

Figure 4.

Viability of 3T3 fibroblast cells and *E. coli* biofilms in the co-culture model after 3 hrs treatment with a) CP-Cap, b) P-Cap, c) SiO_2 NP, and d) peppermint oil at different emulsion concentrations (v/v % of 2 % emulsion). Scatters and lines represent 3T3 fibroblast cell viability. Bars represent $\log_{10}$ of colony forming units in biofilms. The data are average of triplicates and the error bars indicate the standard deviations.

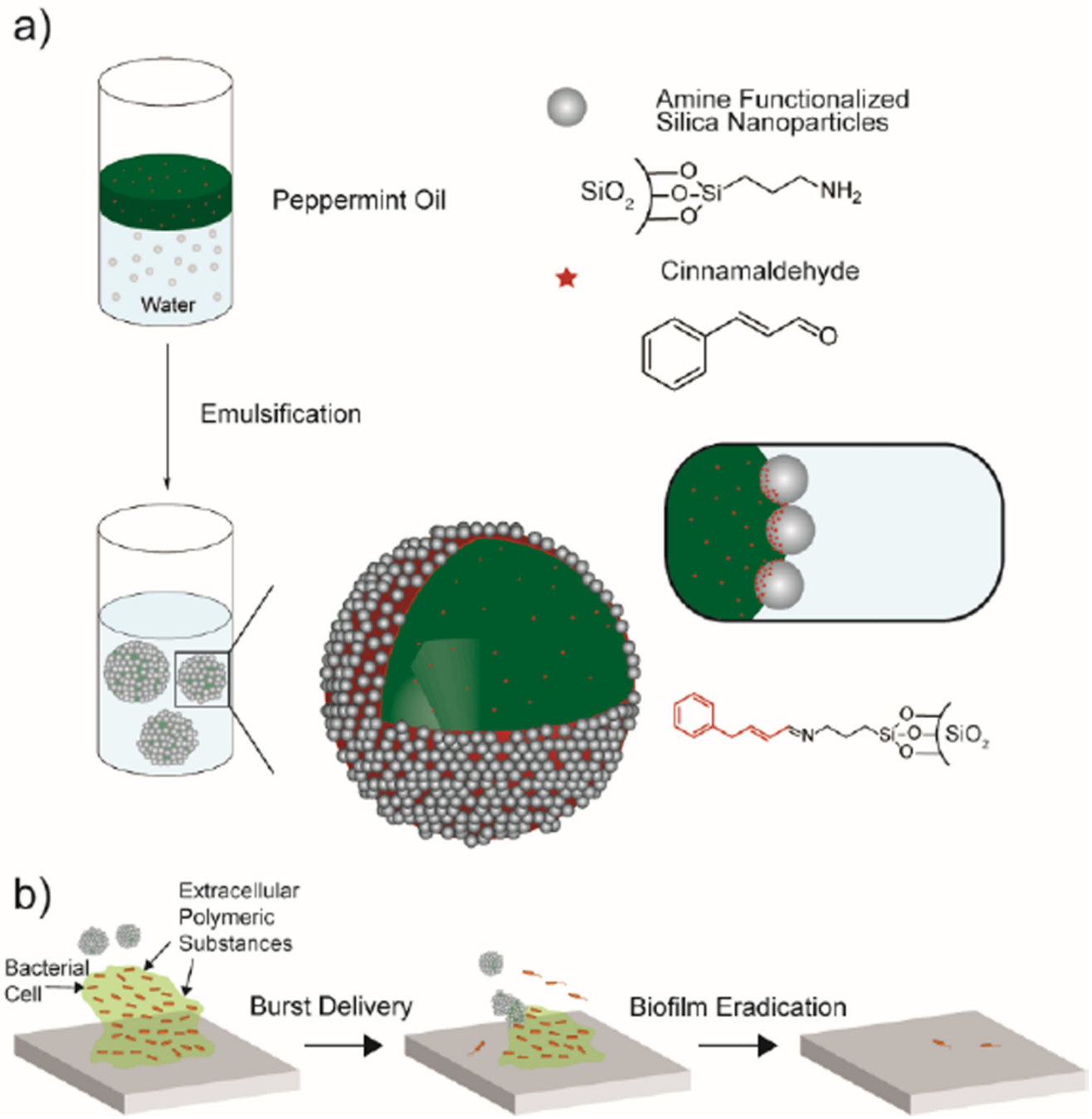

Scheme 1.

a) Schematic depiction of the strategy used to generate antimicrobial capsules. Peppermint oil with dissolved cinnamaldehyde is emulsified into an aqueous suspension of amine functionalized silica nanoparticles. Cinnamaldehyde within the oil reacts with the amines on the nanoparticles at the oil/water interface to create a multimodal delivery vehicle. b) Capsules interact with biofilm through electrostatic complementarity. Capsules release their payload disrupting the biofilm, eliminating the bacteria.